Single-Crystalline Diluted Magnetic Semiconductor GaN:Mn Nanowires**

By *Heon-Jin Choi**, *Han-Kyu Seong*, *Joonyeon Chang*, *Kyeong-Il Lee*, *Young-Ju Park*, *Ju-Jin Kim*, *Sang-Kwon Lee*, *Rongrui He*, *Tevye Kuykendall*, and *Peidong Yang**

Current information technology relies on two independent processes: charge-based information processing (microprocessors) and spin-based data storage (magnetic hard drives).[1–5] The prospect of simultaneously manipulating both charge and spin in a single semiconductor medium is provided by the exciting area of spintronics. Among many others, diluted magnetic semiconductors (DMSs) represent the most promising candidates for such applications.[1–7] Herein we report on the magneto- and optoelectronic properties of single-crystalline diluted magnetic semiconductor nanowires $Ga_{1-x}Mn_xN$ ($x = 0.01$–0.09). These nanowires, which have diameters of ~10–100 nm and lengths of up to tens of micrometers, exhibit ferromagnetism with Curie temperatures (T_Cs) above 300 K and magnetoresistances (MRs) up to 250 K. Spin-dependent electron transport from single-nanowire transistors indicates the homogeneous nature of the ferromagnetic nanowires. Gate-dependent conductance and electroluminescence (EL) from nanowire-based light-emitting-diode structures suggest their p-type characteristics, which might support the theory of hole-mediated ferromagnetism. These ferromagnetic GaN:Mn nanowires represent an important class of nanometer-scale building blocks for spintronics.

Theoretical studies indicate that transition-metal-doped GaN possesses a ferromagnetic transition temperature higher than room temperature due to hole-mediated ferromagnetism,[8] which would be advantageous for many of the proposed spintronic applications. Many experiments have already been carried out to demonstrate such hypotheses,[9–11] although significant controversy exists over the possibility of magnetic-impurity phase separation in many of these thin-film studies.[12–16] Moreover, intrinsic defects in these films originating from the molecular-beam epitaxial growth process may be the Achilles' heel in reaching a fundamental understanding of the ferromagnetism in these materials. On the other hand, the miniaturization of electronic devices represents an ongoing trend for both industrial manufacture and academic research. Among many other possibilities, nanotubes and nanowires are currently being actively explored as possible building blocks for electronic devices with features smaller than 100 nm.[17] The controlled fabrication and fundamental understanding of low-dimensional ferromagnetic semiconductor nanostructures is thus crucial to the development of semiconductor-based spintronic devices and spin-based quantum-computation schemes.

Although progress has been made in the understanding of DMS quantum wells and dots,[1–7] studies of quantum wires are still at a nascent stage. Dimensionality and size are known to play a significant role in determining various properties of the systems.[17] In this regard, a one-dimensional (1D) DMS system at the nanometer scale, i.e., a DMS nanowire, is expected to have interesting magnetoelectronic properties and could be a good candidate for realizing spintronic devices for several reasons. First, nanowires themselves are attractive building blocks for nanometer-scale electronic and optoelectronic devices; second, magnetic nanowires could act as spin filters to supply spin-polarized carrier currents[5] and could also have large magnetic anisotropy energies; third, carriers could be confined in the radial direction of nanowires and, therefore, high carrier concentrations and efficient injection of spin-polarized carriers could be potentially achieved; finally, the single-crystalline nanowires could be used as a model DMS system for exploring the origin of ferromagnetism in these semiconductors by excluding extrinsic effects such as secondary phases.

Synthesis of DMS nanowires represents a challenging issue which has not been reported thus far. To carry out meaningful investigation on DMS nanowires, the ideal wires should be single-crystalline, and the transition-metal dopant must be homogeneously distributed without phase separation. The synthetic challenge resides in the limited transition-metal equilibrium solubility in semiconductors as well as in the intrinsic difficulty in nanocrystal doping. Processes like molecular beam

[*] Prof. H.-J. Choi, H.-K. Seong
School of Advanced Materials Science and Engineering
Yonsei University
Seoul 120-749 (Korea)
E-mail: hjc@yonsei.ac.kr
Prof. P. Yang, R. He, T. Kuykendall
Materials Science Division, Lawrence Berkeley National Laboratory
Department of Chemistry, University of California
Berkeley, CA 94720 (USA)
E-mail: p_yang@berkeley.edu
H.-K. Seong, Dr. J. Chang, K.-I. Lee, Dr. Y.-J. Park
Future Technology Research Division
Korea Institute of Science and Technology
Seoul 136-791 (Korea)
Prof. J.-J. Kim
Department of Physics
Chon-buk National University
Chon-ju 561-756 (Korea)
Prof. S.-K. Lee
Department of Semiconductor Science and Technology
Chon-buk National University
Chon-ju 561-756 (Korea)

[**] This work was supported in part by the Camille and Henry Dreyfus Foundation, the Alfred P. Sloan Foundation, the Beckman Foundation, the Department of Energy, and the National Science Foundation. Work at the Lawrence Berkeley National Laboratory was supported by the Office of Science, Basic Energy Sciences, Division of Materials Science of the U. S. Department of Energy. We thank the National Center for Electron Microscopy for the use of their facilities. H. J. C. thanks Yun-Ki Pyun for technical support. H. J. C. also thanks support from Korea Institute of Science and Technology (E18110) and Center for Nanostructured Materials Technology (04K1501-01710) under 21st Century Frontier R&D Programs of the Ministry of Science and Technology, Korea. J. C. thanks the support from KIST Vision 21 program. J. J. K. thanks the support from Electron Spin Science Center at POSTECH.

 DOI: 10.1002/adma.200401706

ADVANCED MATERIALS

epitaxy (MBE) and implantation have shown limited success in preparing DMSs from group III–V semiconductors, particularly the GaN system.[9–16] These technical difficulties have been successfully overcome in this study, and we were able to prepare single-crystalline GaN:Mn nanowires in a controlled manner via a unique chloride-based chemical vapor transport process.

The nanowires were grown by transporting gallium chloride ($GaCl_3$) and manganese chloride ($MnCl_2$) onto a nickel-coated sapphire or silicon carbide (SiC) substrate under a flow of ammonia (NH_3) at 800 °C.[17,18] To control the Mn concentration in the nanowires, we transported the $GaCl_3$ and $MnCl_2$ by using metallic Ga, Mn, and hydrogen chloride (HCl) gas. Figure 1a shows a typical scanning electron microscopy (SEM) image of the nanowires grown on the substrate. The diameters of these nanowires range from 10 to 100 nm, while the lengths are tens of micrometers. Figure 1b shows a high-resolution transmission electron microscopy (HRTEM) image of an individual nanowire. The perfectly single-crystalline nature, without defects or secondary phase inclusions, can be readily seen in all of the HRTEM images taken of these nanowires. The selected area electron diffraction (SAED) pattern recorded of the wire can be indexed according to the wurtzite GaN structure. The X-ray diffraction (XRD) pattern further confirmed the single-phase nature of these nanowires. Differences in the structural characteristics of $Ga_{1-x}Mn_xN$ nanowires with composition were not observed in XRD and TEM analysis for $x = 0$–0.09. Figure 1c shows the representative Mn concentration determined by energy dispersive X-ray (EDX) spectroscopy analysis on the $Ga_{0.93}Mn_{0.07}N$ nanowires. The average Mn concentration measured from ten nanowires was 7 %, and the Mn dopant was found to be distributed homogeneously within the nanowire lattice.

Electron energy loss spectroscopy (EELS) has been widely used for microanalysis of materials composition. It has been well documented that EELS spectra of transition metals is highly sensitive to the oxidation state of the metal.[19] EELS analysis of the valence state of the Mn dopant in GaN was carried out in reference to the spectra acquired from standard specimens with known cation oxidation states: MnO, Mn_2O_3, and MnO_2. Comparison of the shape and relative intensity ratios of the L_3 and L_2 lines (Fig. 1d) unambiguously shows that the Mn dopants exist as Mn^{2+} cations (d^5 electron configuration) within the GaN matrix. Consequently, it is likely that

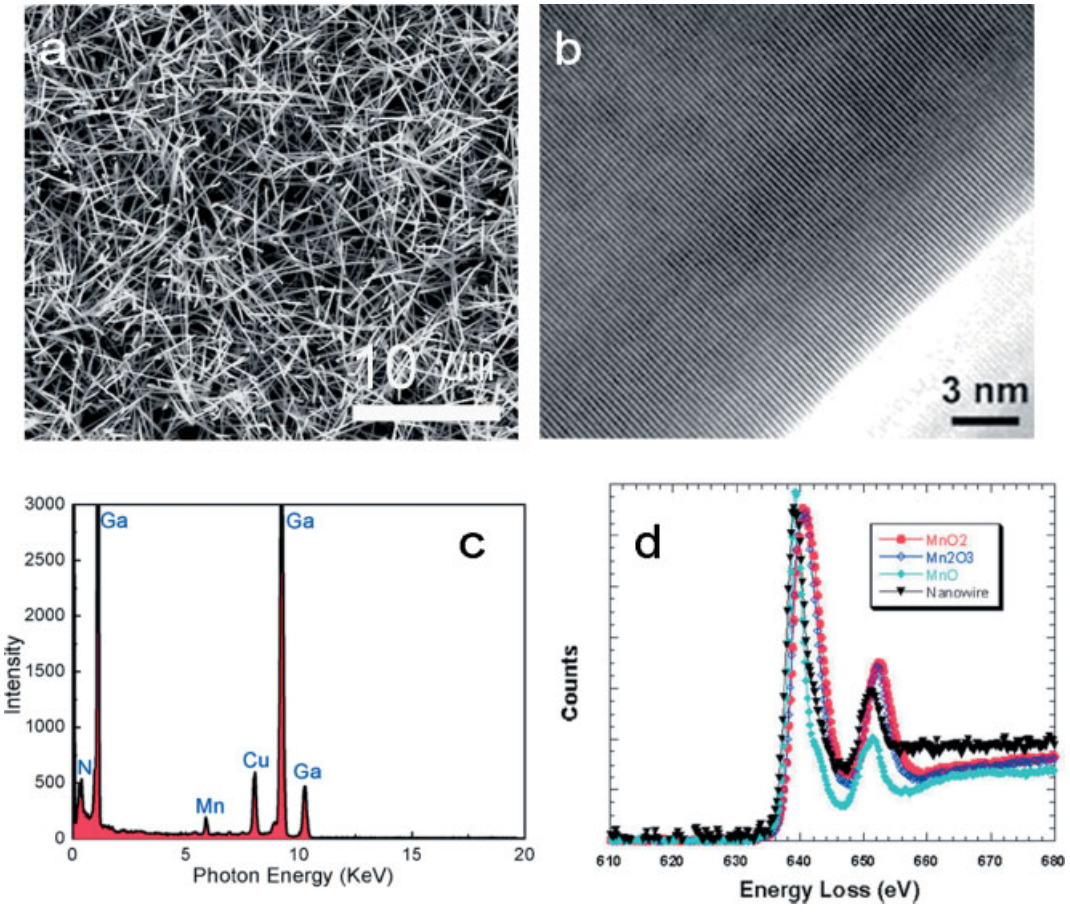

Figure 1. Structure and composition of GaN:Mn nanowires. a) SEM image of the nanowires grown on sapphire substrate. b) HRTEM image of a nanowire. c) EDX spectrum of the nanowire. d) EELS spectra of the GaN:Mn nanowires shown together with the spectra collected from the standard reference samples: MnO, Mn_2O_3, MnO_2.

Mn^{2+} exists as acceptors within the GaN:Mn nanowires produced at high temperature. This argument is further confirmed by our photoluminescence (PL) studies on these GaN:Mn nanowires. The PL spectrum shows the appearance of a broad emission at 2.5–3.2 eV, which matches well with previous GaN:Mn thin-film studies, within which Mn also exists as Mn^{2+}.[20]

Whereas most of the transition-metal-doped DMSs have been prepared by MBE processes at low temperatures to suppress the formation of a secondary phase,[9–16] the GaN:Mn nanowires presented here were prepared by a high-temperature equilibrium vapor transport process. The presence of HCl is considered to be critical in our process. The transported $GaCl_3$, $MnCl_2$, and NH_3 can produce a GaN:Mn crystalline phase.

In this reaction, $GaCl_3$ and $MnCl_2$ serve as thermodynamically favorable transport agents for the formation of a single GaN:Mn phase. Importantly, this process produces single-crystalline GaN:Mn nanowires with absolutely no phase separation or grain boundaries, which have been common problems in most of the previous GaN:Mn thin-film studies.

The magnetic properties of the nanowires were determined using superconducting quantum interference device (SQUID) magnetometry. Figure 2a shows the magnetization loops of a $Ga_{0.93}Mn_{0.07}N$ nanowire sample. The magnetic hysteresis and remanence were clearly observed at 5 K and 300 K, respectively, indicating these GaN:Mn nanowires are ferromagnetic, even at room temperature. This is also reflected in the temperature-dependent magnetization data collected at 0.02 T and 0.5 T (Fig. 2c). Aqua regia treatment of the as-grown nanowires also showed no effect on the magnetic properties. The coercive fields in Figure 2b are ~0.008 T and ~0.004 T for 5 K and 300 K, respectively. Note that the theoretical model of hole-mediated ferromagnetism could explain the high T_C observed in GaN:Mn phases; however, high hole and Mn concentrations (e.g., 3.5×10^{20} cm^{-3} and 5 %, respectively) are required for such a high T_C.[8] We also note the possibility of coexistence of other unknown paramagnetic phases in our ensemble samples used for magnetic measurements. Magneto-transport measurements on individual nanowires, therefore, are critical in order to pin down the intrinsic magnetic properties of these pure GaN:Mn single-crystalline wires.

To determine the type and concentration of carrier, nanowire field-effect transistor (FET) structures were prepared by using as-grown GaN:Mn nanowires. Current–voltage (I–V) curves for different back-gating voltages from a nanowire-based FET structure were measured, which displayed linear I–V characteristics and suggested that the metal–electrical contacts for the device with Ni/Au electrodes were ohmic. A weak gating effect, seen as a conductivity decrease with positively increasing gate voltage (V_g), was observed, which suggests a p-type carrier character for these nanowires. A literature survey indicates that most previous electrical measurements on GaN:Mn thin films have shown that they possess n-type conductance behavior,[9–16,21] which could be attributed to the high density of donor states resulting from intrinsic defects.[13] FET measurements on pure GaN nanowires all show n-type characteristics.

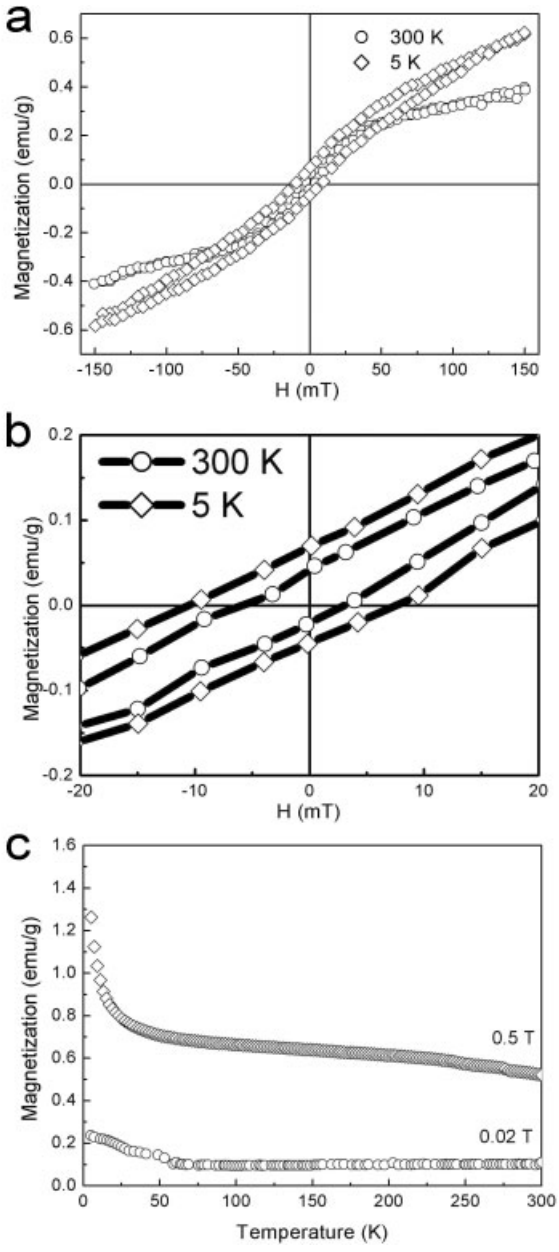

Figure 2. Magnetic properties of GaN:Mn nanowires. a) Magnetization loops of the nanowires measured at 5 K and 300 K (1 emu g^{-1} = 1 A m^2 kg^{-1}). b) Sample magnetization in the low-field region. The hysteresis behavior and remanence were observed at both temperatures. c) Temperature dependence of the magnetization.

I–V measurements of the GaN:Mn nanowires show a low resistivity of 1.1×10^{-2} Ω cm for $V_g = 0$ V at room temperature. This low resistivity, together with a weak gating effect, indicates that a high carrier concentration has been achieved within these nanowires. The mobility is estimated from the transconductance, $dI/dV_g = \mu (C/L^2) V_{sd}$, where μ is the carrier mobility, C is the capacitance, V_{sd} is the source–drain voltage,

ADVANCED MATERIALS

and L is the distance between source and drain. The nanowire capacitance is given by $C \sim 2\pi\varepsilon\varepsilon_0 L/\ln(2h/r)$, where ε is the dielectric constant, ε_0 is the permittivity of free space, h is the thickness of the silicon oxide layer, and r is the nanowire radius. The carrier mobility was estimated as 70 $cm^2 V^{-1} s$. The mobility is low compared to that of bulk and/or thin-film GaN:Mn, which could be explained by a high carrier concentration or enhanced scattering in the nanometer-scale diameter of the nanowire, or both. It is difficult to calculate the carrier density of heavily doped and carrier-confined nanowires due to difficulties in achieving full depletion of carriers by back-gate voltage.[21] Indeed, we observed incomplete depletion in a V_g range of –10 to 10 V. A simple extrapolation leads to a carrier concentration of ca. 2×10^{19} cm^{-3}. This value is higher than that of doped GaN thin films; however, it is an order of magnitude lower than that assumed in the theoretical model (e.g., 3.5×10^{20} cm^{-3}) for a room-temperature T_C.[8]

Importantly, these GaN:Mn nanowires exhibit negative MR up to 250 K. Figure 3 shows the isothermal MR of an individual nanowire measured by four-probe methods. Negative MR (resistance decreases with applied magnetic field) with values of 1.4 % and 0.4 % at 2 K and 250 K, respectively, at 9 T was observed. This MR diminished near room temperature. This type of negative MR has also been observed in (Ga,Mn)As and (Ga,Mn)N epitaxial thin films.[9–16] Such a negative MR can be explained by the reduction of scattering due to aligning of the spins by an applied magnetic field. MR measurements on pure GaN nanowires at similar temperatures and field ranges show no signs of magnetoresistance.

The ferromagnetic nature of the nanowires can be further confirmed by a spin-dependent electron-transport measurement in individual nanowires using ferromagnetic electrodes. The inset of Figure 3d shows a scanning electron microscopy (SEM) image of a nanowire-based tunneling MR device structure used in this study. Ferromagnetic Co electrodes (labeled 2 and 4) and Ti/Au electrodes (1 and 3) were used here. Figure 3d shows the resistance measured between a ferromagnetic Co electrode (electode 2) and a Ti/Au electrode (electrode 3) through a GaN:Mn nanowire at two different bias voltages of 0.6 mV and 2 mV at 4.2 K. The results show clear hysteresis behavior, which are commonly observed in tunneling MR devices. The I–V characteristics at 4.2 K show nonlinear behavior, which implies the formation of tunnel barriers between the electrodes and the nanowire. The typical resistance in the linear region is about 440 kΩ at 4.2 K, and the resistance change, ΔR, is about 9 kΩ at a bias voltage of 0.6 mV, giving a MR change of $\Delta R/R = 1.3$ %. This hysteresis MR was observed up to about 20 K. The resistance of a nanowire with two different metal contacts can be expressed by

$$R = R_{Co/NW} + R_{NW} + R_{NW/Ti} + R_{Co} \quad (1)$$

where R_{Co} and R_{NW} are the resistance of the Co electrode and nanowire respectively, while $R_{Co/NW}$ and $R_{NW/Ti}$ are the tunnel resistances from the Co/nanowire and nanowire/Ti contacts. Among those resistances, $R_{Co/NW}$, R_{Co}, and R_{NW} are the possible origins of the hysteretic MR. R_{Co}, however, has a resistance below 100 Ω, insufficient to explain the magnitude of the MR change (tens of kΩ). We also confirmed that R_{NW} itself did not contribute to the hysteretic MR with control experiments using

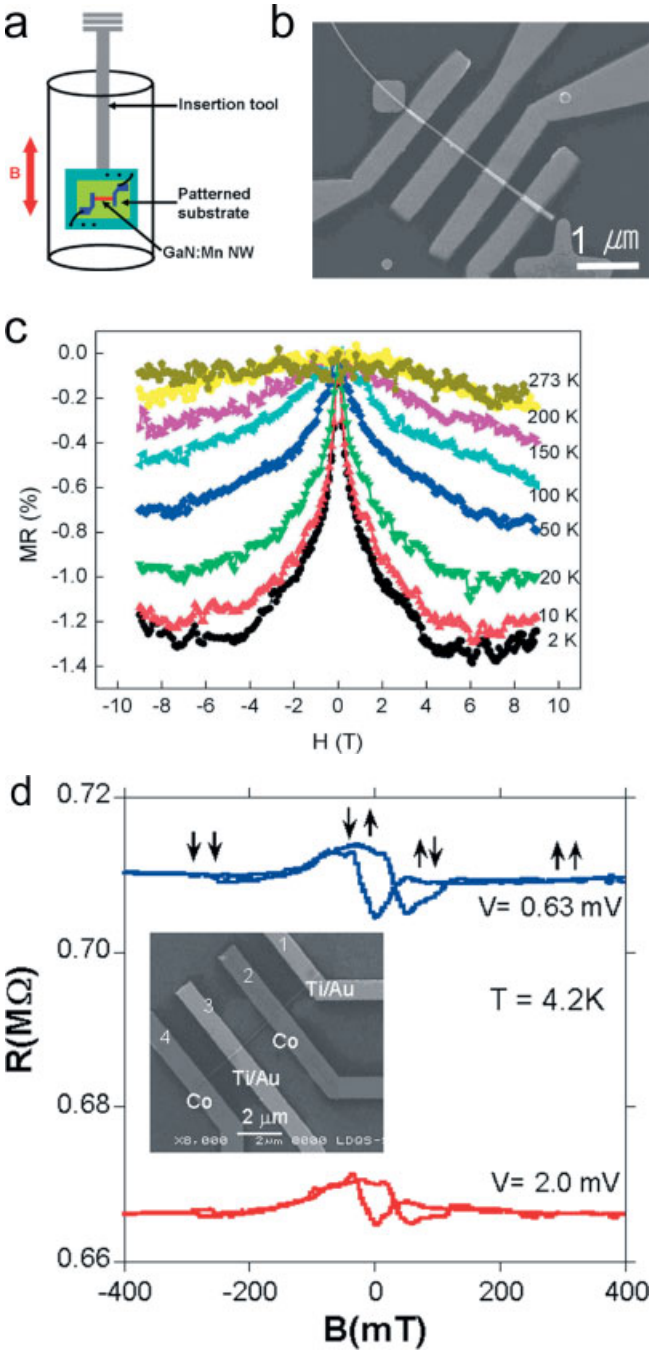

Figure 3. MR of the GaN:Mn nanowires (NWs). a) Schematic illustration of the MR measurement setup. b) SEM image of the nanowire device. c) Magnetoresistance of GaN:Mn nanowire at several different temperatures. d) Resistance change as a function of magnetic field between electrodes 2 and 3 at 4.2 K with bias voltages of 0.63 and 2.0 mV. Inset shows the SEM image of a GaN:Mn nanowire with two ohmic-contacted Ti/Au electrodes (labeled 1 and 3) and two ferromagnetic Co electrodes (2 and 4).

non-magnetic Ti contacts with the nanowire. As a result, the contributions from magnetic contact between Co and the nanowire, $R_{Co/NW}$, is believed to cause the observed hysteretic MR.

Much experimental evidence collected from thin films of GaN:Mn did not support the theory of hole-mediated ferromagnetism, as predicted. However, our measurements suggest that the holes are possibly responsible for both charge transport and ferromagnetic interaction; i.e., our observations made of these single-crystalline GaN:Mn nanowires might support the Zener model of hole-mediated room-temperature ferromagnetism for GaN:Mn.[8] We believe that the perfectly single-crystalline nature of the wires could exclude the effect of structural defects as well as secondary phases (which commonly exist in thin films) and make it possible to observe *intrinsic* ferromagnetism of this material.

Lastly, as a first step towards exploring new spintronic device structures based on DMS nanowires, we have assembled light-emitting diode (LED) structures based on GaN:Mn nanowires. For LED-structure fabrication, quasivertically aligned GaN:Mn nanowires were grown on *n*-SiC (0001) substrates using Ni catalysts (Fig. 4a). Ohmic contacts were achieved by evaporating Ni/Au and Ni bilayers on nanowires and substrates, respectively, followed by rapid thermal annealing. Transport measurements made on nanowire LED struc-

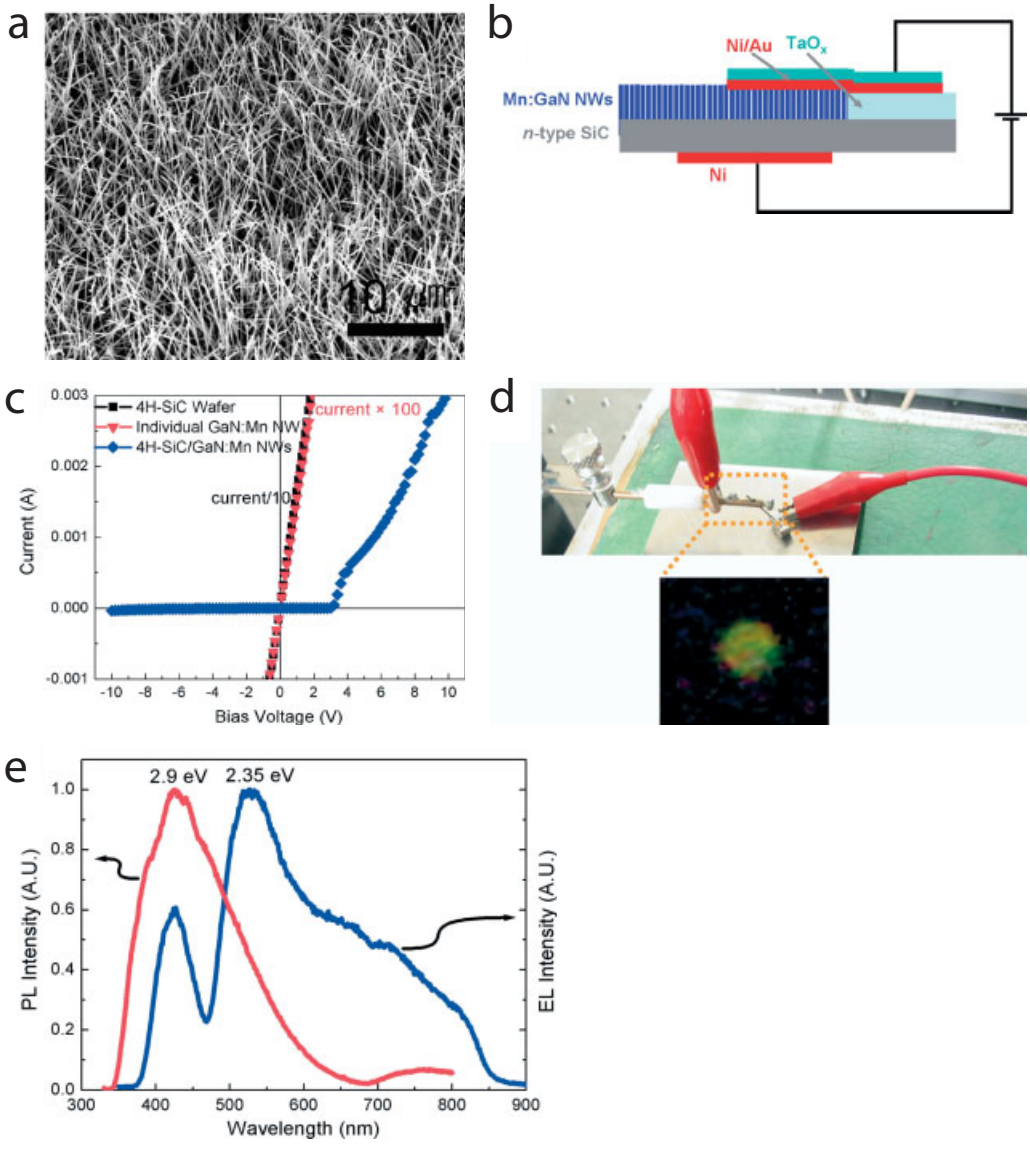

Figure 4. GaN:Mn nanowire LED. a) SEM image of the quasi-vertical nanowire arrays on substrate. b) Schematic illustration of the LED structures. To avoid mechanical failure in the measurement, a TaO_x film was deposited in a small area and metal (Ni/Au) was then evaporated on the nanowire tips through a shadow mask, resulting in a continuous contact layer on the nanowires and the TaO_x insulator. Measurements were carried out by probe contact on the metal layer above the TaO_x layer. c) *I–V* behavior of *n*-SiC substrate/GaN:Mn nanowire junction. d) Image of light emitting interface. Top and bottom images show the device configuration of the nanowire-based LED structure and an optical image of the emitting device, respectively. e) EL spectrum from nanowire LED at 18 V of forward bias, and PL spectrum from GaN:Mn nanowires measured at room temperature using He–Cd laser as excitation source.

ADVANCED MATERIALS

tures show well-defined current rectification, characteristic of p–n diodes (Fig. 4c). Specifically, little current is observed in reverse bias up to –8 V for source–drain bias, and there is a sharp current turn-on at a forward bias of about 3 V. The *I–V* data recorded from the nanowires and substrate were symmetric, and thus we can attribute the rectification to the p–n junction between the nanowires and substrate and not to the junction between the nanowires and metal contacts. Significantly, EL spectra measurements on these junctions show a dominant emission peak centered at 430 nm that is consistent with PL of the nanowires. This EL study further suggests the p-type character of the GaN:Mn nanowires.

Taken together, our simple chloride-based transport approach to preparing single-crystalline GaN:Mn nanowires enables facile doping of transition-metal ions into GaN matrix within these 1D nanostructures. This synthetic success leads to a new class of diluted magnetic semiconductor nanowires with Curie temperatures above room temperature, magnetoresistances near room temperature, spin-dependent transport, and p-type character. These p-type DMS GaN:Mn nanowires may open up new opportunities for fundamental research on the origin of ferromagnetism of diluted magnetic semiconductors. The availability of such nanowires may also open up new opportunities to realize nanometer-scale spintronic and optoelectronic devices such as spin-LEDs, transistors, and ultradense non-volatile semiconductor memory.

Experimental

Nanowire Synthesis and Characterization: GaN:Mn nanowires were synthesized using a Ni catalyst deposited on sapphire or silicon carbide substrates by transporting $GaCl_3$ and $MnCl_2$ under flow of ammonia (NH_3) at 800 °C. To control the Mn concentration in the nanowires, we transported the $GaCl_3$ and $MnCl_2$ using metallic Ga, Mn, and hydrogen chloride (HCl) gas. The composition could be controlled by the amount of HCl gas input.

Device Fabrication: Overall, nanowire-based devices were prepared on a silicon wafer with a 100 nm thick thermally grown SiO_2 layer. An isopropyl alcohol (IPA) solution containing GaN:Mn nanowires was prepared and drop-cast onto a pre-patterned Si substrate. After drying, the location of the nanowire was identified, and the source and drain electrodes were defined by lithography for nanowire-based field-effect-transistor (FET) structures. Prior to the metal-electrode deposition (Ni/Au, 20/50 nm) by thermal evaporation, the nanowires were treated in buffered HF (deionized water/HF 10:1 v/v). Ohmic contacts between the nanowire and the electrodes were achieved using rapid thermal annealing (RTA) at 500 °C for 1 min in Ar. The highly conductive Si layer was used as a global back gate.

Four-probe device structures for magnetoresistance (MR) measurements were prepared as follows: First, the coordinate marks were patterned on a thermally oxidized Si (100) substrate using electron-beam lithography followed by metal deposition (Ti/Au, 20/40 nm) by a direct-current (DC) magnetron sputtering system and a lift-off process. The nanowire solution was dropped onto a pre-patterned Si substrate, and the locations of each nanowire relative to the patterned marks were estimated by atomic force microscopy images. Four electrodes touching a nanowire were defined using electron-beam lithography. Deposition of Au (40 nm) electrodes and lift-off process finally produced a four-probe device. MR measurements were carried out with a Physical Property Measurement System (PPMS) by applying an external magnetic field up to 9 T in the temperature range 2–300 K.

To study spin-dependent transport, an individual nanowire was prepared on an oxidized Si substrate. The patterns for electrical leads were generated by using electron-beam lithography, and then metal (Ti/Au bilayer, 20 and 50 nm thick, respectively) were successively deposited on the contact area by thermal evaporation. Ohmic contacts between the nanowire and the Ti/Au electrodes were achieved by the rapid thermal annealing at 400 °C for 30 s, and the contact resistance was decreased by 20–30 %. After establishing ohmic contacts, ferromagnetic Co metal was deposited onto the pre-patterned nanowire to form magnetic tunnel barrier junctions by thermal evaporation.

For fabrication of light-emitting diode structures, quasi-vertically aligned Mn:GaN nanowires were grown on *n*-SiC (0001) substrates using Ni catalysts. Ohmic contacts were fabricated by evaporating Ni/Au and Ni bilayers on nanowires and substrates, respectively. After metallization of the substrate, a thick TaO_x film was deposited in a small area through a shadow mask where the nanowires were removed. Ni and Au were then evaporated, resulting in a continuous contact layer on the nanowires and the TaO_x insulator. Measurements were carried out by probe contacts on the metal film above the TaO_x.

Received: October 15, 2004
Final version: December 31, 2004
Published online: March 24, 2005

[1] S. D. Sarma, *Nat. Mater.* **2003**, *2*, 292.
[2] S. J. Pearton, C. R. Abernathy, M. E. Overberg, G. T. Thaler, D. P. Norton, N. Theodoropoulou, A. F. Hebard, Y. D. Park, F. Ren, J. Kim, L. A. Boatner, *J. Appl. Phys.* **2003**, *93*, 1.
[3] H. Akinaga, H. Ohno, *IEEE Trans. Nanotechnol.* **2002**, *1*, 19.
[4] T. Dietl, *Semicond. Sci. Technol.* **2002**, *17*, 377.
[5] I. Malajovich, J. J. Berry, N. Samarth, D. D. Awshalom, *Nature* **2001**, *411*, 770.
[6] H. Ohno, *Science* **1998**, *281*, 951.
[7] S. A. Wolf, D. D. Awschalom, R. A. Buhrman, J. M. Daughton, S. von Molnar, M. L. Roukes, A. Y. Chtchelkanova, D. M. Treger, *Science* **2001**, *294*, 1488.
[8] T. Dietl, H. Ohno, F. Matsukura, J. Cibert, D. Ferrand, *Science* **2000**, *287*, 1019.
[9] K. H. Kim, K. J. Lee, D. J. Kim, H. J. Kim, Y. E. Ihm, D. Djayaprawira, M. Takahashi, C. S. Kim, C. G. Kim, S. H. Yoo, *Appl. Phys. Lett.* **2003**, *82*, 1775.
[10] H. Hori, S. Sonoda, T. Sasaki, Y. Yamamoto, S. Shimizu, K. Suga, K. Kindo, *Phys. B (Amsterdam, Neth.)* **2002**, *324*, 142.
[11] M. C. Park, K. S. Huh, J. M. Myoung, J. M. Lee, J. Y. Chang, K. I. Lee, S. H. Han, W. Y. Lee, *Solid State Commun.* **2002**, *124*, 11.
[12] M. L. Reed, N. A. El-Masry, H. H. Stadelmaier, M. K. Ritums, M. J. Reed, C. A. Parker, J. C. Reberts, S. M. Bedair, *Appl. Phys. Lett.* **2001**, *79*, 3473.
[13] M. Zajac, J. Goak, M. Kaminska, A. Twardowski, T. Szyszko, S. Podsiadlo, *Appl. Phys. Lett.* **2001**, *79*, 2432.
[14] Y. Soon, Y. H. Kwon, S. U. Yuldashev, J. H. Leem, C. S. Park, D. J. Fu, H. J. Kim, T. W. Kang, X. J. Fan, *Appl. Phys. Lett.* **2002**, *81*, 1845.
[15] N. Theodoropoulou, A. F. Hebard, M. E. Overberg, C. R. Abernathy, S. J. Pearton, S. N. G. Chu, R. G. Willson, *Appl. Phys. Lett.* **2001**, *78*, 3475.
[16] M. E. Overberg, C. R. Abernathy, S. J. Pearton, N. Theodoropoulou, K. T. McCarthy, A. F. Hebard, *Appl. Phys. Lett.* **2001**, *79*, 1312.
[17] Special issue on "One-Dimensional Nanostructures", *Adv. Mater.* **2003**, *15*, 351.
[18] H. Choi, J. Johnson, R. He, S. Lee, F. Kim, P. Pauzauskie, J. Goldberger, R. Saykally, P. Yang, *J. Phys. Chem. B* **2003**, *107*, 8721.
[19] Z. L. Wang, J. S. Yin, Y. D. Jiang, *Micron* **2000**, *31*, 571.
[20] Y. Shon, Y. H. Kwon, T. W. Kang, X. Fan, D. Fu, Y. Kim, *J. Cryst. Growth* **2002**, *245*, 193.
[21] K. H. Kim, K. J. Lee, D. J. Kim, H. J. Kim, Y. E. Ihm, C. G. Kim, S. H. Yoo, C. S. Kim, *Appl. Phys. Lett.* **2003**, *82*, 4755.

